



Article

# An effective power quality enhancement system for integrated photovoltaic cells utilizing cascaded ANFIS in a unified power quality conditioner

Saritha Kandukuri<sup>1\*</sup>, Ramesh Guguloth<sup>2</sup>, A. Sivakumar<sup>3</sup>, I. Shivasankkar<sup>4</sup>, Ananthan Nagarajan<sup>5</sup>, N. Janaki<sup>6</sup>

<sup>1</sup>Department of Electrical and Electronics Engineering, Eklavya University, Damoh, Madhya Pradesh, 470661

<sup>2</sup>Department of Electrical and Electronics Engineering, Sreenidhi Institute of Science and Technology, Hyderabad, Telangana-501301, India

<sup>3</sup>Department of Electrical and Electronics Engineering, Panimalar Engineering College, Nazerthpattai, Poonamalle, Chennai, 600123, India

<sup>4</sup>Department of Electrical and Electronics Engineering, Sri Manakula Vinayagar Engineering College, Puducherry, 605107, India

<sup>5</sup>Department of Electrical and Electronics Engineering, Vel Tech Multi Tech, Dr. Rangarajan Dr. Sakunthala Engineering College, Chennai-62, India

<sup>6</sup>Department of Electrical and Electronics Engineering, Vels Institute of Science, Technology and Advanced Studies, Chennai, India

## ARTICLE INFO

### Article history:

Received 22 April 2025

Received in revised form

04 June 2025

Accepted 14 June 2025

### Keywords:

Unified Power Quality Conditioner, Artificial Neural Network controller, PV system, Coupled quadratic SEPIC converter Cascaded ANFIS-MPPT

\*Corresponding author

Email address:

[mugatha.saritha@gmail.com](mailto:mugatha.saritha@gmail.com)

DOI: 10.55670/fpll.futech.4.3.16

## ABSTRACT

The arrival of power electronic devices for the control of loads has an effect on the Power Quality (PQ) at the utility grid's distribution side. Meanwhile, PQ problems cause malfunctioning equipment, lost production time, loss of money for industry, inconvenience, and possible damage to household electrical appliances. Thus, the requirement for increased system efficiency is essential. Hence, this study proposes the control of a Unified Power Quality Conditioner (UPQC) in conjunction with a Photovoltaic (PV) system. Shunt and series converters attached back-to-back via a shared DC-link make up the PV-UPQC system. Subsequently, the Artificial Neural Network (ANN) controller reduces PQ problems and simplifies the control complexity. A Coupled quadratic Single Ended Primary Inductor Converter (SEPIC) connects the PV system to UPQC, and the Cascaded Adaptive Neuro Fuzzy Inference System- Maximum Power Point Tracking (ANFIS-MPPT) technique enables the optimization of power extraction from PV sources. The developed approach is implemented using the MATLAB/Simulink platform, and its performance is evaluated for Total Harmonic Distortion (THD), sag, and swell. The results show that the control maintains THD within the B-phase THD of 3.97% and R and Y phase THDs of 4.82% and 4.86%, and also obtained a voltage gain ratio of 1:15; the output levels increase substantially with reduced voltage stresses on the switching devices.

## 1. Introduction

The usage of non-linear loads and unbalanced loads has increased in the modern era due to the expansion of the distribution system and the expansion of industry. PQ problems get inferior during the non-linear load enhancements, and the s distribution grid's structure becomes more intricate [1]. This resulted in issues with PQ, such as distortion and imbalance in the current, sag/swell, and the production of harmonics and imbalance in the system's supply voltage. Voltage quality issues, in particular, have the potential to impair the regular functioning of

sensitive loads that are heavily linked to the distribution grid, resulting in financial losses and other consequences [2]. The essential industrial load is affected by grid voltage disruptions, which result in frequent tripping. In modern years, a number of methods and tools have been established to address PQ problems in distribution networks. Flexible AC Transmission System (FACTS) devices are appealing instruments for improving reactive power control and reliability in transmission systems. These gadgets react swiftly to any disruptions and provide more system flexibility [3].

Abbreviations	
APF	Active Power Filters
ANFIS-MPPT	Adaptive Neuro Fuzzy Inference System- Maximum Power Point Tracking
ANN	Artificial Neural Network
DSTATCOM	Distribution Static Compensator
FACTS	Flexible AC Transmission System
PCC	Point of Common Coupling
PLL	Phase-Locked Loop
PPF	Passive Power Filters
PQ	Power Quality
PV	Photovoltaic
PWM	Pulse Width Modulation
RMSE	Root Mean Square Error
SVC	Static Var Compensator
SEPIC	Single Ended Primary Inductor Converter
THD	Total Harmonic Distortion
UPQC	Unified Power Quality Conditioner

The need for Passive Power Filters (PPF), Active Power Filters (APF), and hybrid power filters has increased due to these limitations, which include fixed compensation, massive size, difficulty in adjusting dependency filter settings, and resonance with source impedance [4-5]. These filters, which are often connected in parallel with the load, are developed to remove current harmonics and adjust for reactive power in the power system. Despite being more affordable and widely accessible, these filters must be retuned to a specific harmonic in order to produce the desired effect, which can lead to overvoltage situations when power demand is lower [6]. The STATCOM is a power electronics device that works by injecting reactive current into the power network's point of common coupling. The primary benefit of the STATCOM is that it does not rely on the Point of Common Coupling's (PCC) voltage level, hence the compensating current is not reduced as the voltage drops. Nevertheless, it has harmonics, high initial costs, and limited steady-state operating modes [7].

By reducing major PQ problems, including sags/swell, harmonics, flickers, and interruptions, the DVR protects the load from failure or tripping; nonetheless, they are ineffective at balancing large-scale voltage sags [8]. Through the regulation of voltage, power factor, and harmonics, the Static Var Compensator (SVC) enhances PQ. However, in order to compensate for surge impedance, SVCs need extra equipment [9]. The PCC provides reactive power to the Distribution Static Compensator (DSTATCOM), which regulates voltage. Nevertheless, its use is restricted by the issue of reactive power injection and power losses [10].

Therefore, this research proposes a UPQC for enhancing the PQ. The UPQC protects the vital loads connected to the distribution system by addressing issues such as neutral and negative sequence currents, harmonic isolation, flow of reactive power at harmonic distortions, voltage disturbances, and harmonic and fundamental frequencies. A PV system is exploited in a UPQC system to leverage the clean, renewable energy developed by solar panels to alleviate PQ issues, which have the highest annual growth curve among the available renewable sources because of their easy installation and limitless supply capacity. However, many PQ problems are also brought on by the extensive integration of PV into the

power grid [11-12]. Thus, the design of solar PV integrated UPQC has many advantages, including enhancing grid PQ and shielding vital loads from grid-side disruptions. Furthermore, the current approaches ignore the problem of voltage instability brought on by PV system intermittency in favour of concentrating solely on the compensating capability and design of UPQC [13]. The conventional converters like Boost [14], Cuk [15], and SEPIC [16] are employed for boosting the voltage of the PV system. However, these conventional converters have a complex structure, high ripple current, and lower efficiency. Therefore, this research develops a coupled quadratic SEPIC converter in the PV-based UPQC system. To enhance the efficacy of the PV system, the MPPT approach is utilized that tracks the highest power from the PV system [17]. The conventional MPPT algorithms like ANN [18], Fuzzy logic [19], and ANFIS [20] have oscillations, undesirable performance, and excessive complexity. Also, the Perturb and Observe (P&O) MPPT [21] method has limitations in terms of oscillations around the Maximum Power Point (MPP), causing a loss in power, its inability to track rapidly changing irradiance conditions, and a lower efficiency with dynamic conditions. Similarly, Incremental Conductance MPPT [22] has a high computation burden, slower tracking with rapidly varying irradiance, and it is also sensitive to noise that causes small oscillations around the MPP. As a consequence, this paper develops a cascaded ANFIS MPPT algorithm for tracking the peak power from the PV system.

### 1.1 Problem statement

PQ issues such as voltage sags, swells, and harmonic distortion are a growing problem in modern power systems with increasing nonlinear loads and distributed energy resources. Poor PQ causes equipment failure, production shutdowns, and financial losses. While UPQC is commonly employed to mitigate these issues, its implementation leads to complex control requirements and wasted energy extraction when combined with renewable sources. This research presents a novel PV-UPQC system, integrated using a Coupled Quadratic SEPIC converter, an ANN controller, and a Cascaded ANFIS-MPPT design, making it possible to improve efficiency and PQ. The key contributions are:

- Integrating the UPQC for mitigating the PQ issues like voltage sag and swell.
- Implementing the Coupled quadratic SEPIC converter for enhancing the low voltage of the PV system to a higher voltage.
- The cascaded ANFIS MPPT is exploited for tracking maximum power from the PV system, which effectively enhances the PV system's efficacy.
- ANN controller approach to minimize control generalization and expand PQ mitigation operations.

### 2. Proposed methodology

The developed PV-based UPQC system is indicated in Figure 1. The three-phase AC supply is connected with a linear/nonlinear load through a UPQC, which has a series and shunt converter with a DC link capacitor. The series converter is exploited for compensating voltage distortions and maintaining voltage stability at the load end. It ensures a seamless power supply for linear or nonlinear loads. Then, the shunt converter is exploited to mitigate current distortions. It ensures that the current drawn by the load remains sinusoidal and balanced, even under nonlinear conditions.

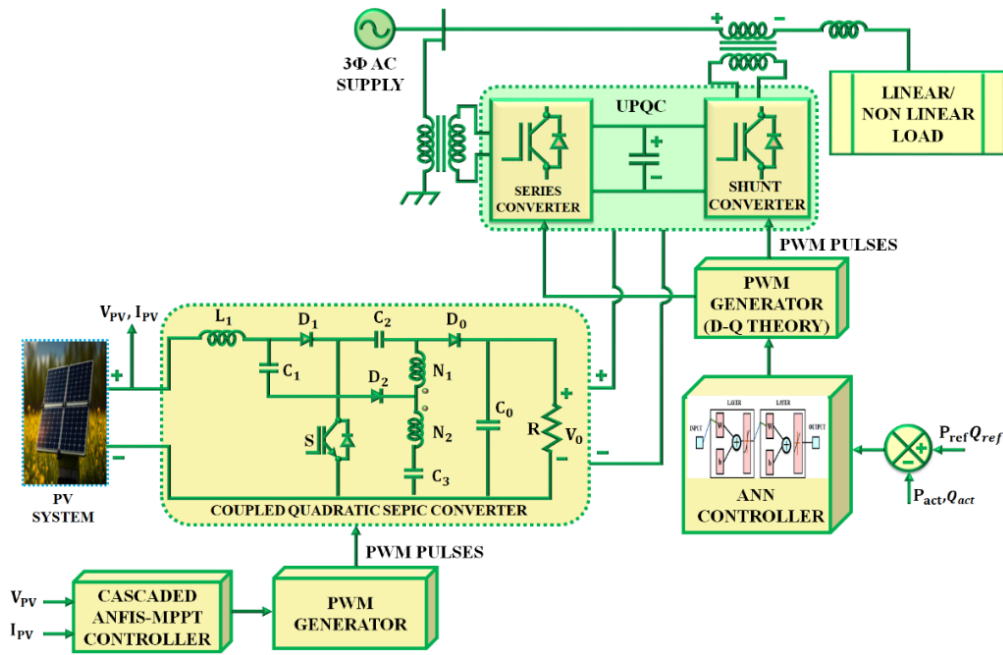


Figure 1. Proposed block diagram

Then, the Pulse Width Modulation (PWM) generator generates PWM pulses for better functioning of the series and shunt converters. To give the power supply to the DC link, the PV system is exploited. Because of the environmental changes, low voltage is generated from the PV system that is improved by utilizing the coupled quadratic SEPIC converter, and its output is supplied to the DC link capacitor. For tracking the peak power from the PV system, the cascaded ANFIS MPPT controller is utilized. Consequently, the ANN controller is exploited to control the function of UPQC, and the PWM generator produces necessary pulses for UPQC. Accordingly, the PQ of the overall system is enhanced with reduced THD.

### 2.1 UPQC

The UPQC is a power conditioning system with shunt and series compensation capabilities that effectively enhances the overall PQ of the system. Figure 2 shows the UPQC's structural diagram. An unbalanced three-phase system's source grid voltage  $V_{grid}(t)$  has fundamental and harmonics in its zero, negative, and positive sequence components. Equation (1) provides the system voltage for the equivalent circuit.

$$V_{grid}(t) = V_{grid+}(t) + V_{grid-}(t) + V_{grid0}(t) + \sum V_{sh} \quad (1)$$

Where  $V_{sh}$  is the shunt converter's voltage and  $V_{grid-}(t)$ ,  $V_{grid+}(t)$  and  $V_{grid0}(t)$  are the negative, positive and zero sequence components. Equation (2) provides the inserted voltage of the series converter.

$$V_{se\_comp}(t) = V_{Load}(t) - V_{grid}(t) \quad (2)$$

Where  $V_{se\_comp}(t)$  is the voltage of the series compensator,  $V_{grid}(t)$  is the source voltage, and  $V_{Load}(t)$  is the load voltage.

The current of shunt compensator is,

$$I_{sh\_comp}(t) = I_{Load}(t) - I_{grid}(t) \quad (3)$$

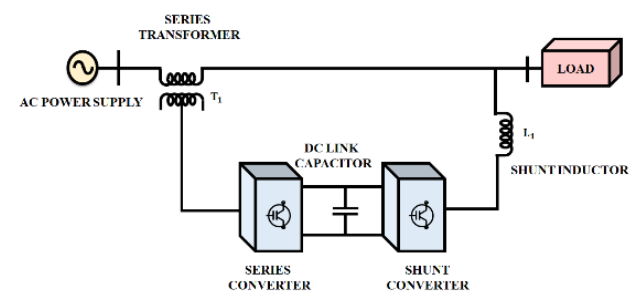


Figure 2. Structure of UPQC system

Where  $I_{sh\_comp}(t)$  is the compensating current,  $I_{Load}(t)$  is the current at the load and  $I_{grid}(t)$  is the current passing over the grid. The current is injected into the grid by the shunt converter.

$$I_{Load}(t) = I_{Load+}(t) + I_{Load-}(t) + I_{Load0}(t) + \sum I_{sh\_comp}(t) \quad (4)$$

Equation (4) provides the distorted load current. Where the load current's positive sequence is denoted by  $I_{Load+}(t)$ , its negative sequence by  $I_{Load-}(t)$ , and its zero-sequence component by  $I_{Load0}(t)$ . The current passing through the shunt compensator is denoted by  $I_{sh\_comp}(t)$ . This system is a three-phase system with a non-linear inductive load. Figure 3 depicts a circuit of the UPQC system.

#### 2.1.1 Series converter

By lowering voltage-related disturbances, including voltage swell and sag, the series converter enhances PQ. The series converter preserves the voltage control, as seen in Figure 4.



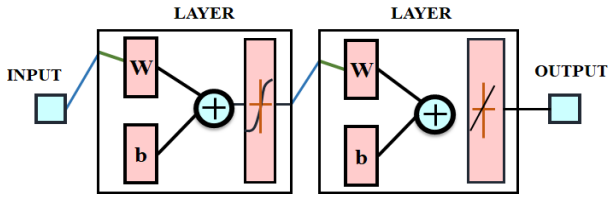


Figure 6. ANN controller

The ANN-based controller reacts quickly and dynamically under a wide range of operating conditions. All of an ANN's inputs are received by the input layer, after which they are processed and stored in the hidden layer. Prior to further processing in the hidden layer, the input weights are multiplied by the bias. Following the completion of specific computations, the results are processed and transmitted to the output layer. ANNs handle data concurrently, which leads to quicker processing speeds than traditional systems. ANN generates reference currents and voltages by combining different learning architectures and principles. This design diagnoses the mean square error and makes both forward and backward weight adjustments until the intended output is attained, and the error is removed if the needed output is not produced. The ANN controller manages both the series and shunt converters in the PV-UPQC system. Particularly, the ANN controller creates the reference signals necessary for both converters to successfully adjust for voltage and current deviations. For the series converter, the ANN aids in adjusting the input voltage to reduce sags, swells, and harmonics, thus stabilising the load-side voltage. The ANN allows the delivery of compensatory currents into the shunt converter, thereby eliminating current harmonics and maintaining a balanced sinusoidal supply. This dual-control feature improves the general efficiency of the UPQC in handling PQ issues. To give the supply to UPQC, the PV system is equipped with a DC-DC converter.

2.3 PV System

The PV system is made up of several PV cells coupled in parallel and series to produce the necessary output voltage and current. Figure 7 displays the circuit of the PV system. The solar temperature and intensity decide the supplied power of the PV system. The expression (1) is the output current generated by the solar cell:

$$I = I_{ph} - I_D - I_{sh} \tag{17}$$

Where  $I$  stands for the PV cell's output current,  $I_{ph}$  is photo-generated current,  $I_D$  is the current of the diode and  $I_{sh}$  is the shunt current. The current that is redirected through the diode is described using the Shockley diode equation as:

$$I_D = I_o \left( \exp \left[ \frac{q(V+IR_s)}{mKT_c} \right] - 1 \right) \tag{18}$$

The current in a PV cell is:

$$I = I_{ph} - I_o \left( \exp \left[ \frac{q(V+IR_s)}{mKT_c} \right] - 1 \right) - \left( \frac{V + IR_s}{R_{sh}} \right) \tag{19}$$

Where  $T_c$  is the absolute temperature,  $R_s$  is the series resistance,  $R_{sh}$  is shunt resistance,  $I_o$  is diode saturation current,  $q$  is elementary charge,  $K$  is the Boltzmann constant,  $m$  is quality factor of diode and  $V$  is the output voltage. Here, the low voltage of PV system is enhanced by a coupled quadratic SEPIC converter.

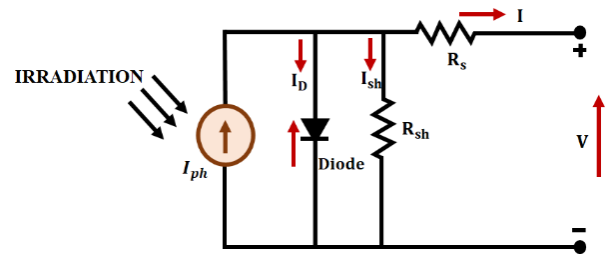


Figure 7. Circuit of the PV system

2.4 Coupled quadratic SEPIC converter

The coupled quadratic SEPIC converter transforms low and intermittent input voltage from the PV system to a higher voltage. Figure 8 reveals the coupled quadratic SEPIC converter. The following presumptions are taken into consideration in order to summarize the converter's principle: all of the components are ideal, the resistance of the capacitors and inductors is minimal; the ON resistance of the  $S$ , the diodes and parasitic capacitances' voltage drop are all very small. The developed converter is operated in 3 modes, as shown in Figure 9 and Figure 10, which represent the functional waveform of the developed converter.

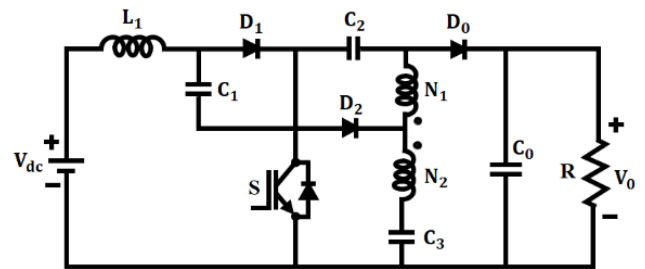


Figure 8. Coupled quadratic SEPIC converter

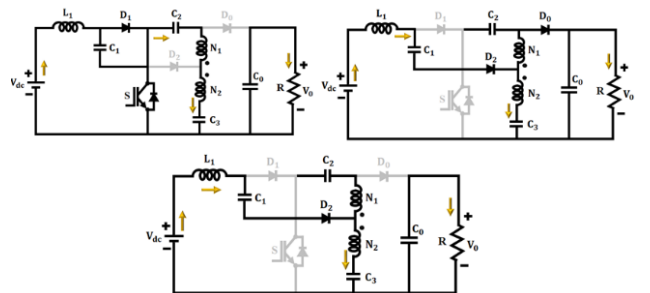


Figure 9. Stages of the developed converter

Mode I

The diode  $D_1$  and switch  $S$  are conducting in this state. Capacitors  $C_3$  and  $C_0$  are reverse biased  $D_2$  and  $D_0$ , which are not conducting. With the current route  $V_{dc} - L_1 - D_1 - S - V_{dc}$ , the input source ( $V_{dc}$ ) energizes inductor  $L_1$ . Through the current path, windings  $N_1$  and  $N_2$  become magnetized as  $N_2 - N_1 - C_2 - S - C_3 - N_2$ . The output capacitor  $C_0$ , which is separated from the DC source, powers the resistive load. The current of  $L_1$  and  $L_M$  increases from  $t_0$  to  $t_1$ .

Mode II

When the power switch  $S$  is turned off and diode  $D_1$  is reverse-biased by capacitor  $C_2$ , in operating mode II.  $L_1$  uses

$V_{dc} - L_1 - C_1 - V_{dc}$  to discharge the energy it has stored in  $C_1$ . Through the  $C_3 - N_2 - N_1 - V_o - C_3$  route, the energy saved in the coupled-inductors is released to the  $C_3$  and load. The current of  $L_1$  and  $L_M$  reduces from  $t_1$  to  $t_2$ .

**Mode III**

In mode III,  $D_o$  is reversed as biased while the power switch is off as a consequence of the leaking inductance effect. The consequence of turning off the diode  $D_o$  is disregarded in converter operation by using the appropriate magnetizing inductance, high coupling coefficient, and low leakage inductance. The voltage relation among windings  $N_1$  and  $N_2$  is:

$$n = \frac{V_{N1}}{V_{N2}} \tag{20}$$

By applying KVL in state 1,

$$V_{L1} = V_{dc} \tag{21}$$

$$V_{Lm} = \frac{V_{C3} - V_{C2}}{n-1} \tag{22}$$

For mode 2,

$$V_{L1} = V_{dc} - V_{C1} \tag{23}$$

$$V_{Lm} = -\frac{V_{C2}}{n} \tag{24}$$

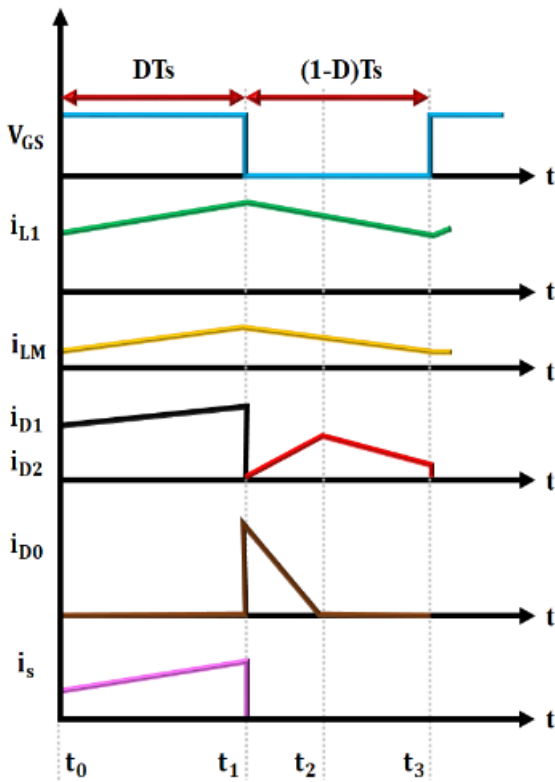


**Figure 10.** Functional waveform of the developed converter

By utilizing the volt-second balance law for the inductors and magnetizing  $L_M$ ,

$$\int_0^{DTs} V_{L1} dt + \int_{DTs}^{T_s} V_{L1} dt = 0 \tag{25}$$

$$\int_0^{DTs} V_{Lm} dt + \int_{DTs}^{T_s} V_{Lm} dt = 0 \tag{26}$$

Where  $T_s$  and  $D$  denote the switching period and duty cycle of the proposed converter.

$$V_{C1} = \frac{1}{1-D} V_{dc} \tag{27}$$

$$V_{C2} = \frac{nD}{(1-D)^2(n-1)} V_{dc} \tag{28}$$

$$V_{C3} = \frac{n-1+D}{(1-D)^2(n-1)} V_{dc} \tag{29}$$

The output dc voltage is:

$$V_o = \frac{n-1+nD}{(1-D)^2(n-1)} V_{dc} \tag{30}$$

The voltage gain is:

$$G = \frac{V_o}{V_{dc}} = \frac{n-1+nD}{(1-D)^2(n-1)} \tag{31}$$

The cascaded ANFIS MPPT controller is exploited for tracking the peak power from the PV system.

**2.5 Cascaded ANFIS MPPT controller**

By continuously modifying the operational parameters, the proposed work uses a cascaded ANFIS MPPT controller to optimize the power output from the PV system. Figure 11 shows a flow chart of the developed controller. Reference voltage and current are produced by the ANFIS controller based on the PV system’s operating state at the time. Important parameters, including temperature, pressure, and the PV system’s output current and voltage, are used as inputs. The membership function fuzzifies the input variables, which are in charge of converting clear input into fuzzy sets so that the ANFIS manages the inherent uncertainty in the behavior of PV systems. Finally, a set of fuzzy rules is developed according to the past data. The relationship between input variables and output is defined by these rules. To make sure the PV system runs at its MPP, the secondary ANFIS controller modifies the developed converter’s duty cycle. The secondary ANFIS receives real-time voltage and current measurements as well as reference values produced by the primary ANFIS controller. The secondary controller controls the duty cycle changes of the converter using a rule-based and fuzzification.

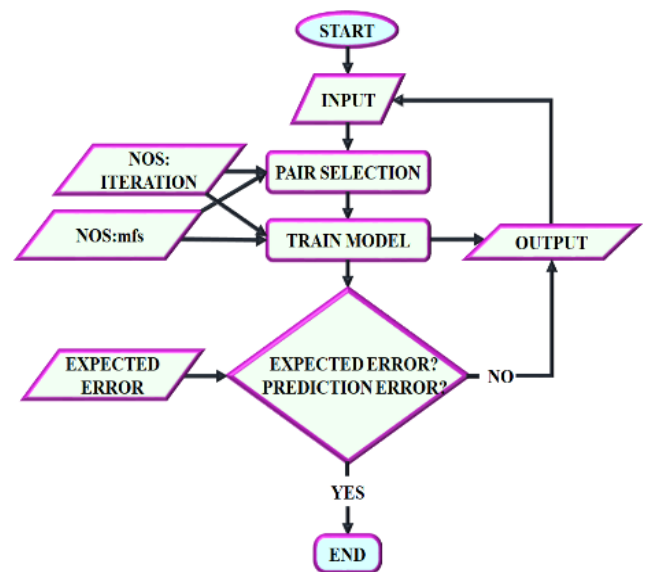


**Figure 11.** Flowchart of cascaded ANFIS-MPPT controller

2.5.1 Pair selection module

By choosing the optimal input variable pairings, the goal is to increase the ANFIS model's accuracy. Each pair of input variables is assessed according to its capacity to reduce the Root Mean Square Error (RMSE) among the actual and expected outputs in a sequential feature selection procedure. An ANFIS model with two inputs is trained and evaluated for every pair. The pairing with the lowest RMSE is chosen.

2.5.2 Training module

Each data pair's RMSE is determined by comparing the predicted and actual outputs. Iterative training is applied to the cascaded ANFIS model till the RMSE is less than a predetermined goal error. The accuracy of the model is improved by using the outputs from each iteration as inputs for the next one. Assume that the four input variables  $Z_1, Z_2, Z_3$  and  $Z_4$ . The defined optimization problem is as follows.

$$input = \{Z_1, Z_2, Z_3, Z_4\} \tag{32}$$

$$input_{pairs} = \{Z_1, Z_3\}, \{Z_2, Z_1\}, \{Z_3, Z_4\}, \{Z_4, Z_1\} \tag{33}$$

The two outputs are the result of  $RMSE_i$  and predicted output  $Y_i$ .

$$RMSE = \sqrt{(A - P)^2} \tag{34}$$

$$RMSE_{A,P} = \left[ \sum_{i=1}^N \frac{(O_{Ai} - O_{Pi})^2}{N} \right]^{1/2} \tag{35}$$

$$f = \frac{\omega_1}{\omega_1 + \omega_2} f_1 + \frac{\omega_2}{\omega_1 + \omega_2} f_2 + \frac{\omega_3}{\omega_2 + \omega_3} f_3 + \frac{\omega_4}{\omega_3 + \omega_4} f_4 \tag{36}$$

The predicted and actual results are denoted as  $P$  and  $A$  while  $N$  is the size and sample. The obtained outputs from  $Y$  and RMSE at the end of the first iteration. After comparing the RMSE and goal error, the subsequent iteration is selected appropriately. The distinctive aspect of this approach is that the outcomes from iterations  $Y_1, Y_2, Y_3$  and  $Y_4$  are exploited as inputs for later iterations. To extract the peak power from the PV panel, the same process is used. The trained ANFIS modules continuously monitor the PV system variables while it is operating. Based on inputs, these modules forecast the required current and voltage, which is utilized to optimize the PV power output. The controller modifies the operating conditions to keep the system running at maximum efficiency.

3. Results and discussion

This section discusses the outcomes of the PV-based UPQC system for voltage swell and sag conditions. The developed research is executed in the MATLAB/Simulink tool, and a performance comparison is included to reveal the efficacy of the developed research. Table 1 depicts the parameter values of the proposed research.

Figure 12 reveals the waveform of the AC source. The voltage of the AC source is 400 V in the starting period, and it is reduced to 280 V. Then, it changed back to 400 V (voltage sag is 120 V). Likewise, the current of an AC source does not maintain a stable value and experiences continuous variations. Both the voltage waveform and the current waveform from the AC source are continuously changing throughout the analysed time frame. Figure 13 represents the waveform of the developed converter. The input voltage of the developed converter is maintained at 72 V in the entire system. In the initial stage, the input current is varied and then sustained at 2500 A throughout the system. The output voltage of the converter is gradually raised and settled at 740

V. Likewise, the output current is randomly changed and maintains a value of 12A.

Table 1. Specification of parameters

Parameter	Specification
<b>AC Source</b>	
Load Resistance	100Ω
Load Inductance	10mH
<b>PV system</b>	
Total Power	10K W
Voltage (Open circuit)	22.6 V
Current (Short circuit)	8.95 A
Maximum Peak Current	8.35 A
Number of panels in series connection	2
Number of panels in the shunt connection	17
<b>Coupled quadratic SEPIC converter</b>	
$L_1$	4.7 mH
$C_1, C_2$ and $C_3$	22 μF
$C_0$	2200 μF
Switching Frequency	10 kHz

Case 1: Voltage sag condition

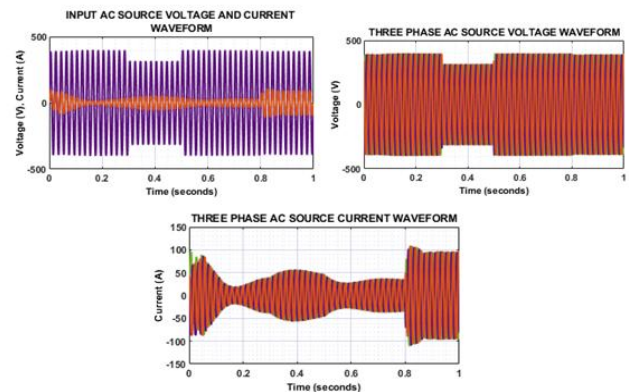


Figure 12. Waveform of the AC source

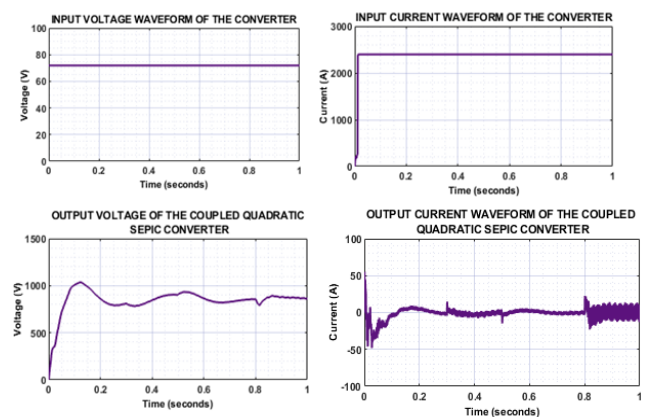


Figure 13. Waveform of the developed converter

Figure 14 shows the output voltage waveform of the Coupled Quadratic SEPIC Converter controlled by a Cascaded ANFIS MPPT Controller. The output voltage stabilizes at 320 V, suggesting a fast response and proper regulation of voltage at the output by the controller.

The waveform of UPQC for the voltage sag condition is represented in Figure 15. The 3 $\phi$  reference voltage for the series converter is randomly changed, and it increased to 80 V with small fluctuations. Then, the 3 $\phi$  reference current is initially altered and is enhanced to a value of 40 A. Consequently, the power factor improved during the time frame that considering, stabilizing at 1, indicating the voltage and current are in sync. The waveform of the load is displayed in Figure 16. The constant voltage of 450 V and stable load current of 35 A is sustained in the entire system stability throughout the testing. Thus, the developed PV-UPQC is effective in increasing the PQ on the source and load sides.

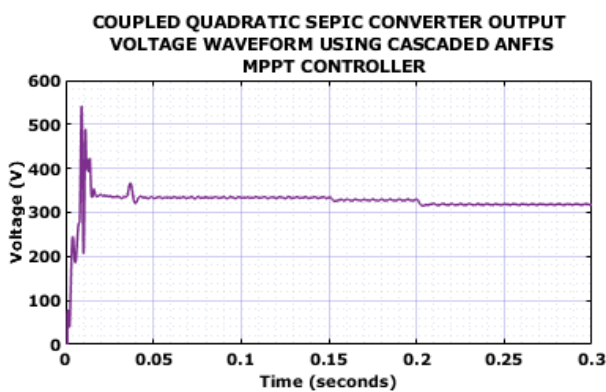


Figure 14. Waveform of developed converter output voltage using cascaded ANFIS MPPT controller

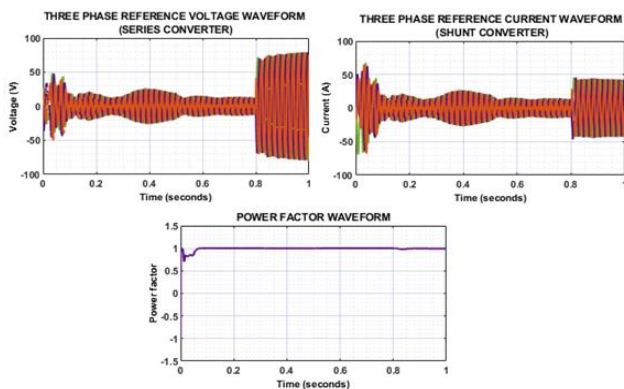


Figure 15. Waveform of UPQC

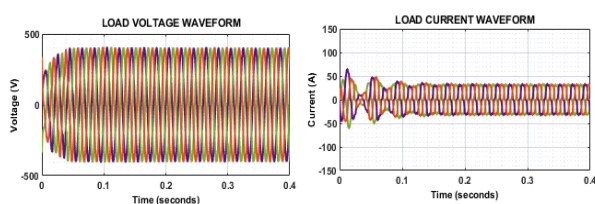


Figure 16. Waveform of load

**Case 2: Voltage swell condition**

Figure 17 illustrates the waveform of the AC source under a voltage swell condition. The source voltage is 400 V, and it increased to 450 V. Finally, it sustained at 400V, and it is influenced by the PQ issue with a voltage swell of 50 V. The source current continues to vary due to PQ issues, and because both the source voltage and current are continuously changing, the source current maintains these continual variations. Figure 18 indicates the waveform of the developed converter under a voltage swell condition. The input voltage is sustained at a stable value of 72 A in the entire system. Similarly, the input current is sustained at a value of 2400 A throughout the system. Then, the converter's output voltage is randomly varied and settled at a value of 880 V with little variation. Finally, the output current is varied arbitrarily in the whole system.

The waveform of UPQC for the voltage swell condition is seen in Figure 19. Initially, the reference voltage of the series converter is 10 V, and it increased to 80 V (that is, the voltage swell is 70 V). Also, the reference current of the shunt converter is 10 A, and it increased to 40 A. Then, the power factor exhibits changes at the beginning due to system changes, but as the time frame transitions, and the power factor stabilizes at the value of 1. The waveform of load voltage and current is depicted in Figure 20. The load voltage is sustained at a value of 450 V, and the load current is settled at 35A for stable operation of the system. The stabilization of the load current and voltage makes a substantial difference in the reliability and operation of the power system.

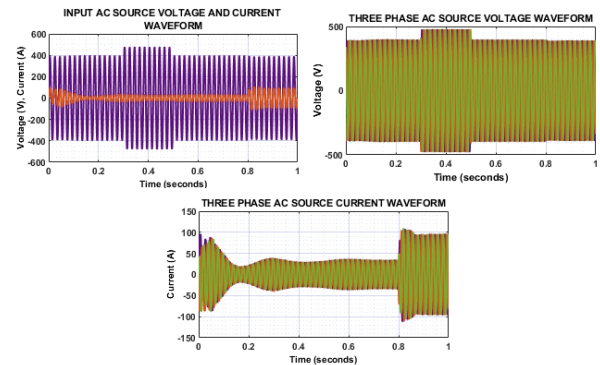


Figure 17. Waveform of the AC source

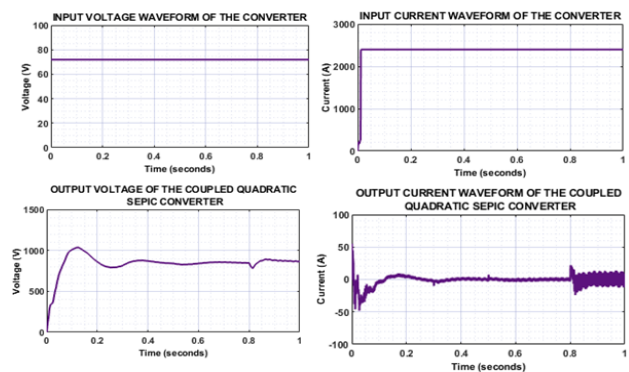


Figure 18. Waveform of the developed converter

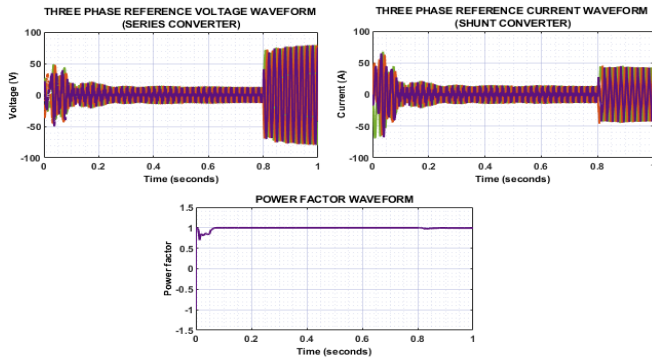


Figure 19. Waveform of UPQC

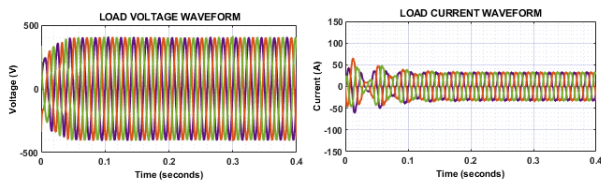


Figure 20. Waveform of load

THD waveforms presented on the three R, Y, and B phases are illustrated in Figure 21. The B phase had the lowest THD of 3.97%, followed by the R and Y phases at 4.82% and 4.86% respectively, which shows that the presented harmonics were adequately reduced, resulting in an improvement in PQ.

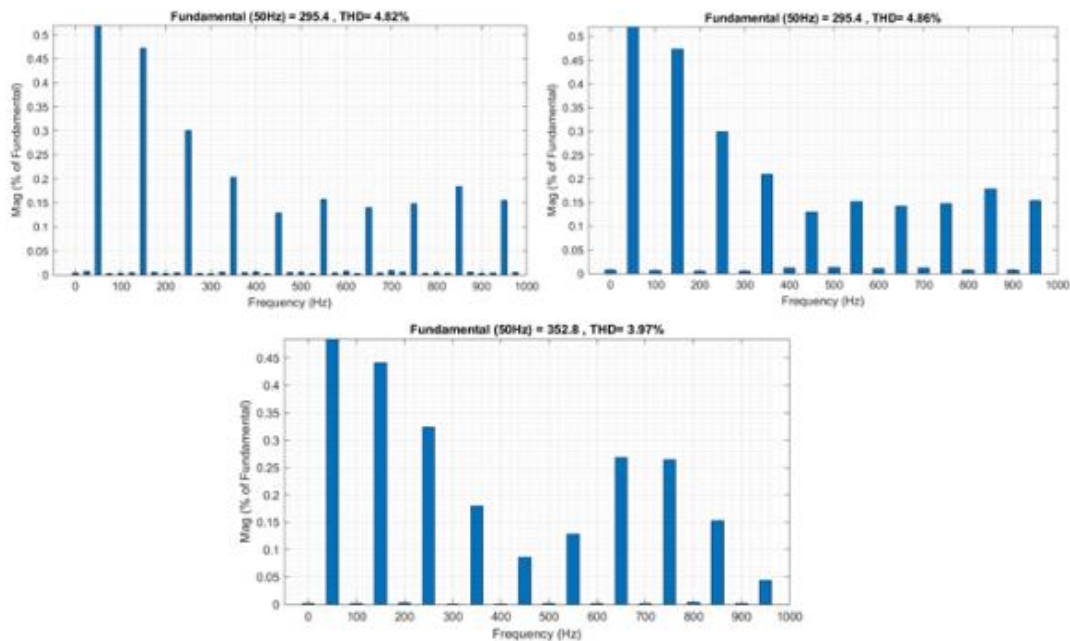


Figure 21. Waveform of THD

The analysis of voltage gain, improved high gain [23], Non-isolated buck-boost [24], and developed converter is depicted in Figure 22. The developed converter attains the highest voltage gain compared to other approaches, ensuring the overall performance of the system is enhanced. Figure 23 displays the comparison of voltage stress for the developed, switched LC-based high-gain [25] and improved high-gain [23] converter. The developed converter has the lowest voltage stress compared to other approaches, indicating that the efficacy of the system is enhanced. The technical benefits of this converter, such as the increased voltage gain and lower voltage stress, support its use in applications needing high DC-DC conversion, and also support overall output quality improvements, reduced voltage ripple, and increased energy efficiency, which all justify using this design in renewable energy systems, including PV applications.

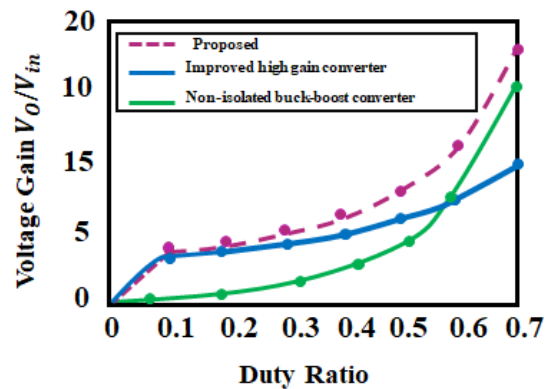


Figure 22. Analysis of voltage gain

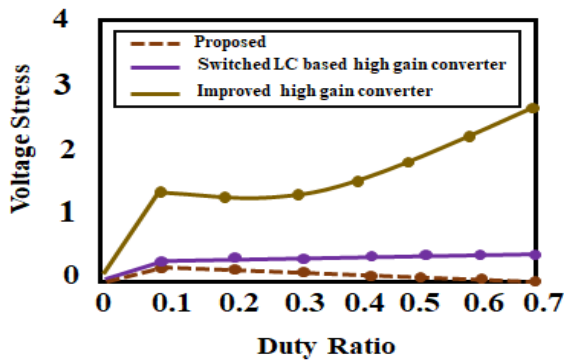


Figure 23. Analysis of voltage stress

The analysis of Grid current THD (%) for R, Y, and B phases for NN [26] and the developed control approach is illustrated in Figure 24. The developed approach demonstrates a reduction in THD compared to NN control across R, Y, and B phases, indicating better harmonic suppression and enhanced PQ.

Figure 25 compares the tracking efficiency of listed MPPT techniques. The proposed method has an efficiency of 98.90%, higher than both ANFIS (97.71%) [27] and Fuzzy (97%) [19], thus proving that it extracts more power under the same conditions than both these techniques. The proposed method demonstrates that it achieved improved tracking efficiency over ANFIS-based and Fuzzy-based MPPT methods, and superior performance.

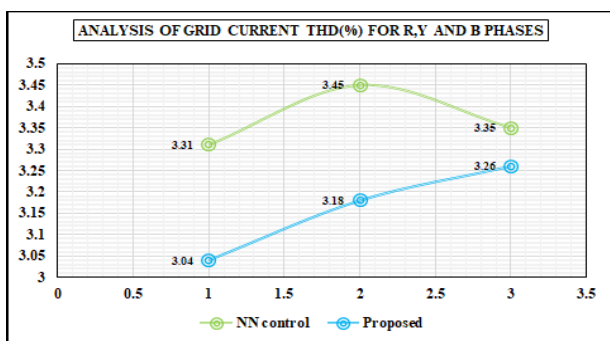


Figure 24. Analysis of grid current THD (%) for R, Y and B phases for unbalanced load conditions

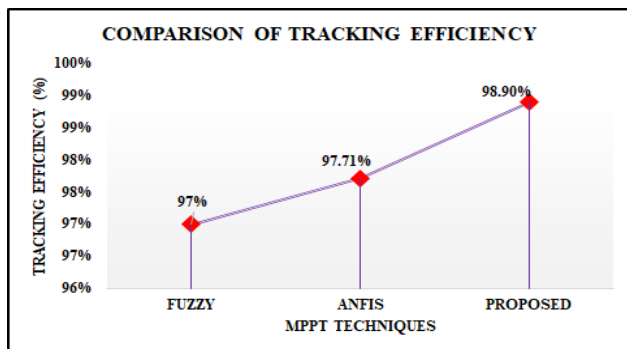


Figure 25. Comparison analysis of tracking efficiency

#### 4. Conclusion

This research presents a novel UPQC system with an ANN controller to diminish PQ problems and offset the load demand in PV systems. As a result, the PV-UPQC provides a superior solution for electrical distribution systems' PQ issues. By eliminating current harmonics, reducing voltage fluctuation, lowering the THD level in accordance with IEEE standards, and improving PQ, the ANN control system offers superior control. Since the PV is an intermediate power source, connecting it directly to the UPQC results in voltage instability, which is resolved by utilizing a coupled quadratic SEPIC converter with better efficacy. Consequently, the cascaded ANFIS MPPT is also exploited for tracking the peak power from the PV system with better tracking efficiency. The series converter compensates for voltage sags, swells, and harmonics, ensuring a stable voltage supply. Then, the shunt converter mitigates current harmonics, corrects power factor, and balances load currents. The results of the MATLAB simulation demonstrate that the developed PV-UPQC system effectively raises the PQ of the source voltage and load current with the lowest THD.

#### Ethical issue

The authors are aware of and comply with best practices in publication ethics, specifically with regard to authorship (avoidance of guest authorship), dual submission, manipulation of figures, competing interests, and compliance with policies on research ethics. The author adheres to publication requirements that the submitted work is original and has not been published elsewhere.

#### Data availability statement

Datasets analyzed during the current study are available and can be provided upon a reasonable request from the corresponding author.

#### Conflict of interest

The authors declare no potential conflict of interest.

#### References

- [1] S. J. Alam and S. R. Arya, "Control of UPQC based on steady state linear Kalman filter for compensation of power quality problems," in Chinese Journal of Electrical Engineering, vol. 6, no. 2, pp. 52-65, 2020. <https://doi.org/10.23919/CJEE.2020.000011>
- [2] C. Jiang and S. Zhang, "Power Quality Compensation Strategy of MMC-UPQC Based on Passive Sliding Mode Control," In IEEE Access, vol. 11, pp. 3662-3679, 2023. <https://doi.org/10.1109/ACCESS.2022.3229893>
- [3] K. Sarita, S. Kumar, A. S. Vardhan, R. M. Elavarasan, R. K. Saket, G. M. Shafiullah and E. Hossain, "Power Enhancement With Grid Stabilization of Renewable Energy-Based Generation System Using UPQC-FLC-EVA Technique," in IEEE Access, vol. 8, pp. 207443-207464, 2020. <https://doi.org/10.1109/ACCESS.2020.3038313>
- [4] S. R. Arya, S. J. Alam and P. Ray, "Optimized PI Gain in UPQC Control Based on Improved Zero Attracting Normalized LMS," In CPSS Transactions on Power Electronics and Applications, vol. 9, no. 2, pp. 242-251, 2024. <https://doi.org/10.24295/CPSSTPEA.2024.00007>
- [5] S. K. Yadav, A. Patel and H. D. Mathur, "PSO-Based Online PI Tuning of UPQC-DG in Real-Time," in IEEE Open Journal of Power Electronics, vol. 5, pp. 1419-

- 1431, 2024.  
<https://ieeexplore.ieee.org/document/10643265>
- [6] J. Yu, Y. Xu, Y. Li and Q. Liu, "An Inductive Hybrid UPQC for Power Quality Management in Premium-Power-Supply-Required Applications," In IEEE Access, vol. 8, pp. 113342-113354, 2020.  
<https://doi.org/10.1109/ACCESS.2020.2999355>
- [7] A. Fouad, H. Kotb, K. M. AboRas, H. B. ElRefaie, M. Alqarni, A. M. Baqasah and A. H. Yakout, "Enhancing Grid-Connected DFIG's LVRT Capability Using Dandelion Optimizer Based the Hybrid Fractional-Order PI and PI Controlled STATCOM," in IEEE Access, vol. 12, pp. 120181-120197, 2024.  
<https://doi.org/10.1109/ACCESS.2024.3427008>
- [8] N. Abas, S. Dilshad, A. Khalid, M. S. Saleem and N. Khan, "Power Quality Improvement Using Dynamic Voltage Restorer," In IEEE Access, vol. 8, pp. 164325-164339, 2020. <https://doi.org/10.1109/ACCESS.2020.3022477>
- [9] C. Gong, W. K. Sou and C. S. Lam, "H $\infty$  optimal control design of static var compensator coupling hybrid active power filter based on harmonic state-space modeling," CPSS Transactions on Power Electronics and Applications, vol. 6, no. 3, pp. 227-234, 2021.  
<https://doi.org/10.24295/CPSTPEA.2021.00021>
- [10] K. H. Tan, M. Y. Li and X. Y. Weng, "Droop Controlled Microgrid With DSTATCOM for Reactive Power Compensation and Power Quality Improvement," In IEEE Access, vol. 10, pp. 121602-121614, 2022.  
<https://doi.org/10.1109/ACCESS.2022.3223352>
- [11] R. Rudraram, S. Chinnathambi and M. Mani, "A Novel Intelligent Neural Network Techniques of UPQC with Integrated Solar PV System for Power Quality Enhancement," International Journal of Electronics and Telecommunications, vol. 69, 2023.  
<http://dx.doi.org/10.24425/ijet.2023.146514>
- [12] S. S. Dheeban and N. B. Muthu Selvan, "ANFIS-based power quality improvement by photovoltaic integrated UPQC at distribution system," IETE Journal of Research, vol. 69, no. 5, pp. 2353-2371, 2023.  
<https://doi.org/10.1080/03772063.2021.1888325>
- [13] K. S. Kavin, P. Subha Karuvelam, M. Devesh Raj and M. Sivasubramanian, "A Novel KSK Converter with Machine Learning MPPT for PV Applications," Electric Power Components and Systems, pp. 1-19, 2024.  
<https://doi.org/10.1080/15325008.2024.2346806>
- [14] K. Salim, M. Asif, F. Ali, A. Armghan, N. Ullah, A. S. Mohammad and A. A. Al Ahmadi, "Low-stress and optimum design of boost converter for renewable energy systems," Micromachines, vol. 13, no. 7, pp. 1085, 2022. <https://doi.org/10.3390/mi13071085>
- [15] Z. Haider, A. Ulasyar, A. Khattak, H. S. Zad, A. Mohammad, A. A. Alahmadi and N. Ullah, "Development and analysis of a novel high-gain CUK converter using voltage-multiplier units," Electronics, vol. 11, no. 17, pp. 2766, 2022.  
<https://doi.org/10.3390/electronics11172766>
- [16] A. Prakash and C. Naveen, "Combined strategy for tuning sensor-less brushless DC motor using SEPIC converter to reduce torque ripple," ISA transactions, vol. 133, pp. 328-344, 2023.  
<https://doi.org/10.1016/j.isatra.2022.06.045>
- [17] K. S. Kavin, P. S. Karuvelam, M. Matcha and S. Vendoti, "Improved BRBFNN-based MPPT algorithm for coupled inductor KSK converter for sustainable PV system applications," Electrical Engineering, pp. 1-23, 2025. <https://doi.org/10.1007/s00202-025-02952-9>
- [18] N. F. Ibrahim, M. M. Mahmoud, A. H. Al Thaiban, A. B. Barnawi, Z. S. Elbarbary, A. I. Omar and H. Abdelfattah, "Operation of grid-connected PV system with ANN-based MPPT and an optimized LCL filter using GRG algorithm for enhanced power quality," IEEE Access, 2023. <https://doi.org/10.1109/ACCESS.2023.3317980>
- [19] K. Ullah, M. Ishaq, F. Tchier, H. Ahmad and Z. Ahmad, "Fuzzy-based maximum power point tracking (MPPT) control system for photovoltaic power generation system," Results in Engineering, vol. 20, pp. 101466, 2023. <https://doi.org/10.1016/j.rineng.2023.101466>
- [20] S. A. Ibrahim, A. Nasr and M. A. Enany, "Maximum power point tracking using ANFIS for a reconfigurable PV-based battery charger under non-uniform operating conditions," IEEE Access, vol. 9, pp. 114457-114467, 2021.  
<https://doi.org/10.1109/ACCESS.2021.3103039>
- [21] Rudraram, Ramesh, Sasi Chinnathambi, and Manikandan Mani. "PV Integrated UPQC with Intelligent Control Techniques for Power Quality Enhancement." International Journal of Electrical and Electronics Research 11, no. 1 (2023): 202-212.
- [22] Asoh, Derek Ajesan, Brice Damien Nouns, and Edwin Nyuysever Mbinkar. "Maximum power point tracking using the incremental conductance algorithm for PV systems operating in rapidly changing environmental conditions." Smart Grid and Renewable Energy 13, no. 5 (2022): 89-108.
- [23] S. Ahmad, M. Nasir, J. Dąbrowski and J. M. Guerrero, "Improved topology of high voltage gain DC-DC converter with boost stages," Int. J. Electron. Lett, vol. 9, no. 3, pp. 342-354, 2021.  
<https://doi.org/10.1080/21681724.2020.1744040>
- [24] A. Sarikhani, B. Allahverdinejad and M. Hamzeh, "A nonisolated buck-boost DC-DC converter with continuous input current for photovoltaic applications," IEEE J. Emerg. Sel. Topics Power Electron, vol. 9, no. 1, pp. 804-811, 2021.  
<https://doi.org/10.1109/JESTPE.2020.2985844>
- [25] A. Kumar, Y. Wang, X. Pan, M. Raghuram, S. K. Singh, X. Xiong and A. K. Tripathi, "Switched-LC based high gain converter with lower component count," IEEE Trans. Ind. Appl., vol. 56, no. 3, pp. 2816-2827, 2020.  
<https://doi.org/10.1109/TIA.2020.2980215>
- [26] O. E Okwako, Z. H. Lin, M. Xin, K. Premkumar and A. J. Rodgers, "Neural network controlled solar PV battery powered unified power quality conditioner for grid connected operation," Energies, vol. 15, no. 18, pp. 6825, 2022. <https://doi.org/10.3390/en15186825>
- [27] E. Touti, M. Aoudia, C. H. Hussaian Basha, and I. M. Alrougy, "A Novel Design and Analysis Adaptive Hybrid ANFIS MPPT Controller for PEMFC-Fed EV Systems," International Transactions on Electrical Energy Systems, vol. 2024, no. 1, pp. 5541124, 2024.

